A MELTING RATE MODEL BASED ON EXTRUSION DATA

Stephen J. Derezinski, *Eastman Kodak Company*

Abstract

To design an extruder screw for a given polymer, the barrel length for melting is needed for a given flow rate and speed. The melting rate needed for calculating the length is given through the conservation laws in cylindrical coordinates based on defined fundamental average parameters. Extrusion machine data are used to calculate the functions of the parameters. Results based on polyethylene data are given.

Background

Detailed distributed analytical models [1,2] have been developed for melting with elaborate experimental freezeout data for verification. A laboratory technique for measuring melting under compacting stress was introduced [3], and it was further developed [4] and modeled [5]. Many versions of a distributed model for melting are available [6], each with its own set of assumptions and technique. Conversely, the model developed here uses the performance data of operating extruders to comprehensively establish average general terms of the energy equation that control the melting process.

Model

Domain of Melting: The extruder is divided into three domains (volumes), which are the feed, melting, and pumping domains. The lengths of the extruder that pertain to each domain are defined *portions.* Portions are determined by thermodynamics and not by geometrical changes (as typically are *sections* of the screw).

Figure 1 shows the melting portion of the extruder to begin at axial position L_f, where the first melting of the polymer occurs (usually on the barrel). The end of the melting portion is reached at axial position L_m, where the average enthalpy (and temperature) of the polymer are those of the fully melted polymer.

Mass Balance: Solid and melt flow will exist at any point, but the net flow in the axial direction is constant at any cross section (see Figure 2). Therefore,

$$\dot{m} = \int_0^{2\pi}\int_{R_S}^{R} \rho v_a r dr d\theta = \text{constant}. \tag{1}$$

Energy Balance: Figure 2 shows the enthalpy, heat transfer, and energy generation terms used for the energy balance. An energy equation is now developed in general terms that can be determined from extruder data.

Integrals around the circumference and through the depth of the channel are summed to give the balance as

$$\frac{d}{dz}\int_0^{2\pi}\int_{R_S}^{R}(\rho v_a h) r dr d\theta = R\int_0^{2\pi}\dot{q}_B d\theta + \int_0^{2\pi}\dot{q}_C R_S d\theta + 2\dot{q}_F\frac{(R-R_C)}{\sin\phi} + \int_0^{2\pi}\int_{R_S}^{R}\dot{e} r dr d\theta. \tag{2}$$

An average enthalpy for the solid-melt flow at a cross section of the channel is defined as

$$\bar{h} \equiv \frac{\int_0^{2\pi}\int_{R_S}^{R}(\rho v_a h) r dr d\theta}{\dot{m}}. \tag{3}$$

Equations 2 and 3 give the axial melting energy distribution as

$$\dot{m}\frac{d\bar{h}}{dz} = R\int_0^{2\pi}\dot{q}_B d\theta + \int_0^{2\pi}\dot{q}_C R_S d\theta + 2\dot{q}_F\frac{(R-R_C)}{\sin\phi} + \int_0^{2\pi}\int_{R_S}^{R}\dot{e} r dr d\theta. \tag{4}$$

The rate of energy generation per unit volume is a comprehensive factor for the mechanical work by the screw that is defined here as $\dot{e}(r,\theta,z)$. It includes the surfaces of the channel and barrel where viscous shear under solid compression has been shown to be a major source of energy [1-5]. It includes the energy generated in the melting that occurs when no or little solid compression exists, such as during solid breakup [7] or during solid bed acceleration [2]. It also includes energy generated in the flight clearance [8] and within the solid by the work of compression [9].

The energy generation can be assumed to approach viscous heat generation of fully melted polymer as melting reaches completion. This is represented by

$$\lim_{z\to L_m}\dot{e} = \eta\dot{\gamma}^2. \tag{5}$$

Therefore, this formulation for energy generation of melting can provide a smooth mathematical transition between the two-phase melting portion and the fully melted portion of the extruder.

Equation 4 is integrated over length to give

$$\dot{m}\int_f^m d\bar{h} = \int_{L_f}^{L_m}\left\{ 2\pi R\dot{q}_B + \int_0^{2\pi}\dot{q}_C R_S d\theta + 2\dot{q}_F\frac{(R-R_C)}{\sin\phi} + \int_0^{2\pi}\int_{R_S}^{R}\dot{e} r dr d\theta \right\} dz. \tag{6}$$

The average power per barrel-area for the entire melt portion is defined as

$$\overline{\dot{P}}_m \equiv \frac{1}{2\pi R \Delta L_m}\int_{L_f}^{L_m}\int_0^{2\pi}\int_{R_S}^{R} \dot{e} r dr d\theta dz , \quad (7)$$

where melting portion length is given by

$$\Delta L_m = L_m - L_f , \quad (8)$$

and the barrel area for the melting portion is then given as

$$A_m = 2\pi R \Delta L_m . \quad (9)$$

The assumption is made that the screw is at steady state temperature so that the sum of the integrals of heat transfer with the screw (channel and flights) is zero. The average heat flux over the entire melting portion length is then defined as

$$\overline{\dot{q}} \equiv \frac{1}{\Delta L_m}\int_{L_f}^{L_m} \dot{q}_B dz . \quad (10)$$

Substituting equations 8 to 10 into equation 6 and completing the integration with the aid of the definition given by equation 7, the basic energy equation for average melting rate per barrel-area is

$$\boxed{\overline{\Omega} \equiv \frac{\dot{m}}{A_m} = \frac{\overline{\dot{q}} + \overline{\dot{P}}_m}{(\overline{h}_m - \overline{h}_f)}} . \quad (11)$$

Parameters from Data

Equation 11 shows three basic melting terms; 1) average melting rate per unit barrel-area, 2) average heat transfer per unit barrel-area, and 3) average power per unit barrel-area. It will be shown that melting rate and power functions can be determined from extrusion data. Equation 11 can then be used to calculate heat transfer functions.

First, data for speed, rate, motor power, barrel temperatures, exit temperature, and pressure for polyethylene are assembled for a variety of extruders and screws as given in the Table. Data for the rheology are shown in Figure 3. Enthalpy and melting point of the polymers are also obtained.

	D, mm	Polymer	CR	v_0, mm/s	T_B, °C
1	114	A	5.0	0.66	304
2	114	B	4.7	0.94	299
3	114	C	4.4	0.66	263
4	203	D	4.1	0.69	232
5	203	D	3.3	0.69	227
6	203	E	4.1	0.65	288
7	63.5	[1]	2.9	0.24	177,204,232

A math model [10,11] is used to calculate the length and power of the *pumping portion*. The length is that which is needed to increase the bulk temperature from the melting point to the measured exit temperature at the measured rate and speed. Similarly, a feed model [12] is used for the *feed portion* to obtain its length, power, and temperature. The melting portion length and power are then found by subtracting those calculated for the feed and pumping portions from the total measured values of the operating extruders. The total screw powers are assumed to be 85% of the motor powers in all cases to account for losses in the drive. An exception is [1] where the melting length was determined from freezeout samples, and the power was modeled.

Melting Rate: The average melting rate, $\overline{\Omega}$, is found by dividing the measured flow-rate by the barrel area for melting, as determined from above. Figure 4 shows the melting rate versus the rotational velocity, ωR, of the screw. Average melting rate increases with velocity, and a maximum value of nearly 0.3 kg/s-m^2 is shown.

Data and calculations for polyethylene [13] show that local melting rates at 0.5 m/s range between 0.35 and 0.75 kg/s-m^2 under 3.45 mPa compressive stress. Figure 4 shows average melting rate at 0.5 m/s to be about 0.15 kg/s-m^2. High compressive stress of [13] would only be present in part of the melting portion (as shown in Fig. 1), so the lower average melting rates of Figure 4 are expected for the total melting portion of the extruder.

Power Generation: The power generation, $\overline{\dot{P}}_m$ in kW/m^2, is calculated from the data by dividing the screw power for the melting portion by its barrel area. The power generation (kW/m^2) is plotted as a function of rotational velocity of the screw, v=ωR (m/s), in Figure 5, and an exponential correlation is shown as

$$\overline{\dot{P}}_m = 110(v)^{1.57} . \quad (12)$$

A function of velocity can be expected because the screw simulation data for polyethylene [13] indicates that the shear stress for melting is independent of surface temperatures above 220 °C. Data for Figure 5 were for barrel zones above 220 °C, except Tadmor [1]. Therefore, even though various extruders, screws, and barrel zone temperatures were used, an exponential correlation of screw power to velocity was obtained.

The exponent for the correlation in equation 12 is 1.57. The exponential for power generation for a shaft turning in an annulus versus speed for a power-law melt is 1+n. Therefore, the power-law exponent pertinent to Figure 5 is n=0.57, which is typical of the polyethylene's used for the data shown in Figure 3.

Heat Transfer: Equation 11 is solved for heat transfer to give

$$\overline{\dot{q}} = \overline{\Omega}(h_m - h_f) - \overline{\dot{P}}_m . \quad (13)$$

Data for melting rate, $\overline{\Omega}$, from Figure 4 and data of power, $\overline{\dot{P}}_m$, from Figure 5 are used to give the heat transfer results of equation 13. They are plotted in Figure 6 as a function of rotational velocity of the screw. The data for each machine are linear with velocity, but they occur at different levels of screw velocity.

The slopes of heat transfer versus velocity of Figure 6 are similar, so the level of velocity for each machine is defined by the intercept, v_0, at zero heat transfer. At these conditions the melt is gaining heat with the barrel over some part of the melting portion, and it is loosing the same amount of heat over the remaining part of the melting portion. The net heat transfer is zero even though the process is not adiabatic. So called "autogenous" conditions [1] exist between the melt and the barrel.

Values of "autogenous velocity" for Figure 6 are given in the previous table. They are subtracted from the screw velocities to give a relative abscissa for the heat transfer data and used to replot the heat transfer of Figure 6 in Figure 7. The heat transfer data (kW/m^2) by linear regression is given as a function of relative velocity (m/s) from Figure 7 as

$$\bar{q} = -120.5(v - v_0)\,. \tag{14}$$

The table shows autogenous velocity to be greater for higher barrel zone temperatures in the melting portion. Observation of the table and consideration of the viscosity data (Figure 3) also indicate that lower viscosity increases the autogenous velocity. Other factors that were not controlled for the data, such as compression ratio (shown) and pressure, are also likely to influence the autogenous velocity.

<u>Temperature:</u> A bulk melt-phase temperature, T, is defined as the average temperature of the melt next to the barrel needed to transfer heat with the barrel. It is based on a heat transfer coefficient [8] and defined by the relationship

$$\int_{L_f}^{L_m} U(T - T_B)dz = \bar{q}\Delta L_m\,. \tag{15}$$

This temperature is assumed equal to the melting point of the polymer at the beginning and end of the melting portion as shown in Figure 1. Therefore,

$$T_{L_f} = T_m \text{ , and} \tag{16}$$

$$T_{L_m} = T_m\,. \tag{17}$$

The net heat transfer from equation 15 with constant barrel temperature and heat transfer coefficient requires the integral of the temperature to be constant, or

$$\int_{L_f}^{L_m} T dz = (T_B + \frac{\bar{q}}{U})\Delta L_m\,. \tag{18}$$

The rate of change of temperature at the beginning of the melting portion is assumed to be that of the end of the feed portion, and it is stated as

$$\left.\frac{dT}{dz}\right|_{L_f} = C_f\,. \tag{19}$$

Finally, the temperature at the end of the melting portion is assumed to be at a local minimum because the temperature will increase in the pumping portion. Therefore,

$$\left.\frac{dT}{dz}\right|_{L_m} = 0\,. \tag{20}$$

A fourth-order polynomial equation is assumed to approximate the bulk melt-phase temperature function that satisfies the five conditions of equations 16-20. Figure 8 shows autogenous and melt-cooling temperatures simulated for a 203-mm diameter screw. Autogenous conditions occur at 61 rpm and require that only a constant heat transfer coefficient be assumed. For a melt cooling condition of -50 kW/m^2, a heat transfer coefficient of 1700 W/m^2-K was assumed. Maximum bulk melt temperatures of about 310 ^oC and 360 ^oC are predicted with the barrel temperature of 232 ^oC.

Polyethylene Melting Rate Equation

As an example, equations 11, 12, and 14 are now used to produce a function for average melting rate of the given polyethylene's and extruders. First, a feed model [12] is used to obtain the enthalpy, $\bar{h}_f$ (kJ/kg), of the resin entering the melting portion. The exiting enthalpy, $\bar{h}_m$, must be known for the polymer at its melting point. Melting rate (kg/s-m^2) is then given as a function of velocity (m/s) with equations 11, 12, and 14 as

$$\bar{\Omega} = \frac{-120.5(v - v_0) + 110(v)^{1.57}}{(\bar{h}_m - \bar{h}_f)}\,. \tag{21}$$

Melting length is found by dividing the flow rate by the melting rate and the circumference as

$$\Delta L_m = \frac{\dot{m}}{2\pi R\bar{\Omega}}\,. \tag{22}$$

Finally, the bulk melt-phase temperature at a given speed can be found from the fourth-order polynomial approximation and the heat transfer of equation 14 subject to the conditions of equations 16-20.

Conclusions

1) A method has been developed with the energy equation, a feed model, and a pumping model to correlate extrusion data for melting rate, heat transfer, and screw power with rotational velocity for the polymer melting portion of an extruder.

2) A screw velocity for autogenous heat-transfer with the barrel in the melting portion is defined, and it is a key reference value for the model.

3) A bulk-average melt temperature for heat transfer with the barrel is defined, and a method for approximating it with a fourth-order polynomial function of length is shown.

Nomenclature

A Area

C_f	$(dT/dz)_f$ at the end of the feed portion
D	Diameter
$\dot{e}$	Energy generation per unit volume
F	Force
h	Enthalpy
L	Axial position
L_f	End feed, beginning of melting portion
L_m	End of melting portion
$\dot{m}$	Mass flow rate
$\dot{P}$	Power generation per unit area
$\dot{q}$	Heat transfer per unit area
Q	Total heat transfer
r	Radial coordinate
R, R_S	Radii, barrel and screw
T	Temperature
U	Heat transfer coefficient
v	Rotational screw velocity
v_a	Axial velocity
v_0	Autogenous velocity
z	Axial coordinate
$\dot{\gamma}$	Shear rate
Δ	Differential increment
η	Viscosity
θ	Rotational coordinate
ρ	Density
σ	Stress
τ	Shear stress
ϕ	Helix angle
ω	Rotational screw speed
$\overline{\Omega}$	Average melting rate per unit area

Subscripts

B	Barrel
C	Channel
f	Feed
F	Flight
m	Melted
S	Screw
θ	Rotational position

References

1. Tadmor, Zehev and I. Klein, *Engineering Principles of Plasticating Extrusion*, Van Nostdrand Reinhold Company, 1970, pp. 79-183.

2. Donovan, R. C. "A Theoretical Melting Model for Plasticating Extruders," *Polymer Engineering and Science*, May, 1971, Vol. 11, No. 3, pp. 247-257.

3. Vermeulen, J. R., Ph.M. Gerson, and W. J. Beek, "The Melting of a Bed of Polymer Granules on a Hot Moving Surface," *Chemical Engineering Science*, 1971, Vol. 26, pp. 1445-1455.

4. Chung, C. I., W. J. Hennessey, and M. H. Tusim, "Frictional Behavior of Solid Polymers on a Metal Surface at Processing Conditions," *Polymer Engineering and Science*, Vol. 17, No. 1, January 1977, pp. 9-20.

5. Mount, E. M. III, J. G. Watson and C. I. Chung, "Analytical Melting for Extrusion: Melting Rate of Fully Compacted Solid Polymers," *Polymer Engineering and Science*, August, 1982, Vol. 22, No. 12, pp. 729-737.

6. Lindt, J. T., "Mathematical Modeling of Melting of Polymers in Single Screw Extruders: A Critical Review," *Conference Proceedings, ANTEC '84*, Society of Plastic Engineers, 1984, pp. 73-76.

7. Rauwendaal, C., "Dispersed Solids Melting Theory," *Conference Proceedings, ANTEC '93*, Society of Plastic Engineers, 1993, pp. 2232-2237.

8. Miller, J. D. and D. H. White, "Heat Transfer in the Transition Section of a Plasticating Extruder," *Conference Proceedings, ANTEC '74*, Society of Plastic Engineers, 1974, pp. 243-246.

9. Derezinski, S. J., "Compressibility of the Resin Solid Feed Bed in Extrusion," *Conference Proceedings, ANTEC '88*, Society of Plastic Engineers, 1988, pp. 105-108.

10. Derezinski, S. J. "Calculating Power of Extruder Melt Sections," *Journal of Materials Processing & Manufacturing Science*, Vol. 6, No. 1, July 1997, pp. 71-77.

11. Derezinski, S. J. "Heat Transfer Coefficients in Extruder Melt Sections," *Conference Proceedings, ANTEC '96*, Society of Plastic Engineers, 1996, pp. 417-421.

12. Derezinski, S. J., "Control Volume Analysis of Feed Flow in Extruders," *Conference Proceedings, ANTEC '98*, Society of Plastic Engineers, 1998, pp. 142-147.

13. Kim, Y. S., C. I. Chung, S. Y. Lai, T. I. Butler, and K. S. Hyun, "Melting Behavior of Different Types of Low Density Polyethylene's and Screw Design Considerations," *Conference Proceedings, ANTEC '96*, Society of Plastic Engineers, 1996, pp. 216-221.

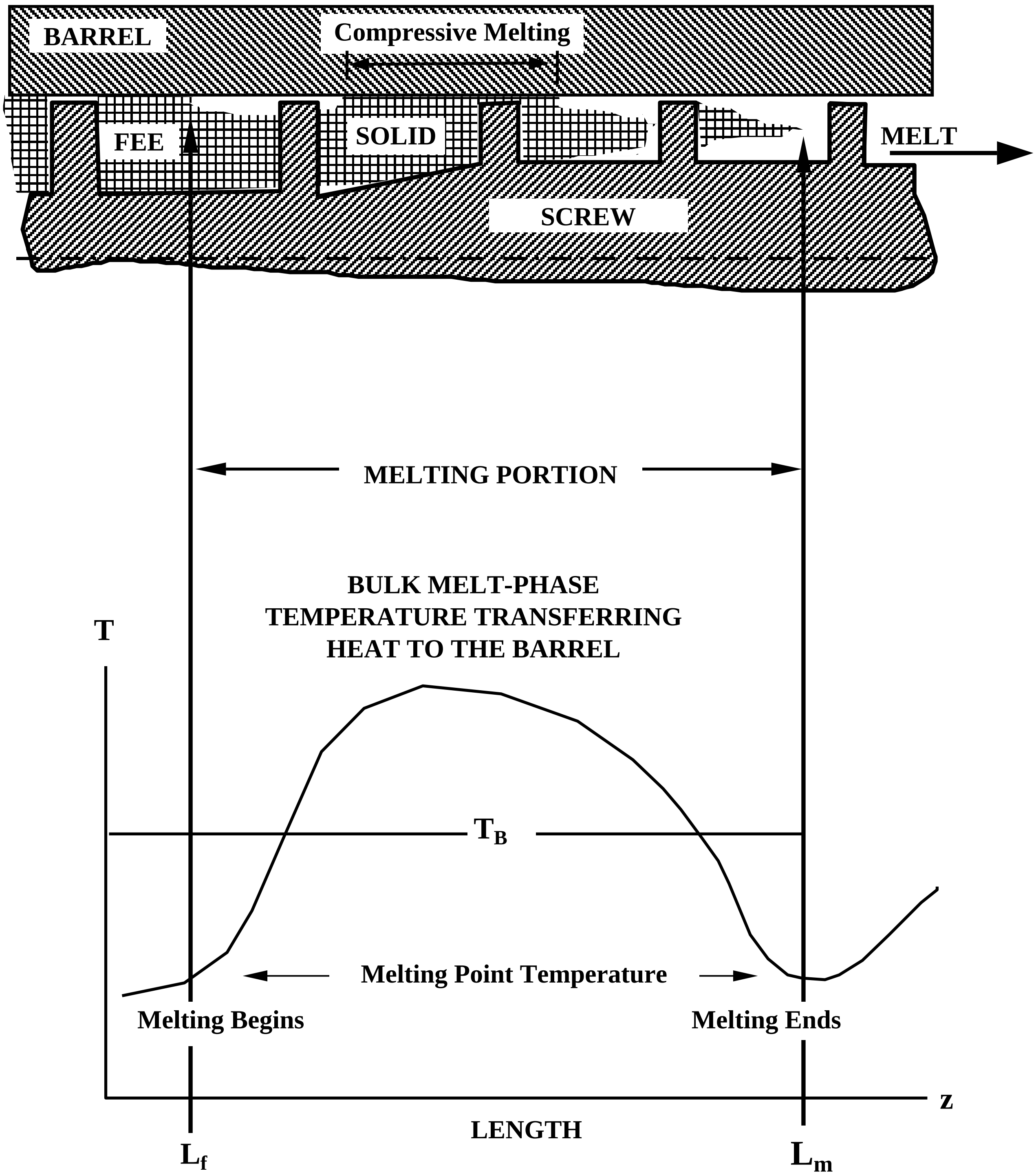

Figure 1. Schematic for the Melting Portion of the Extruder.

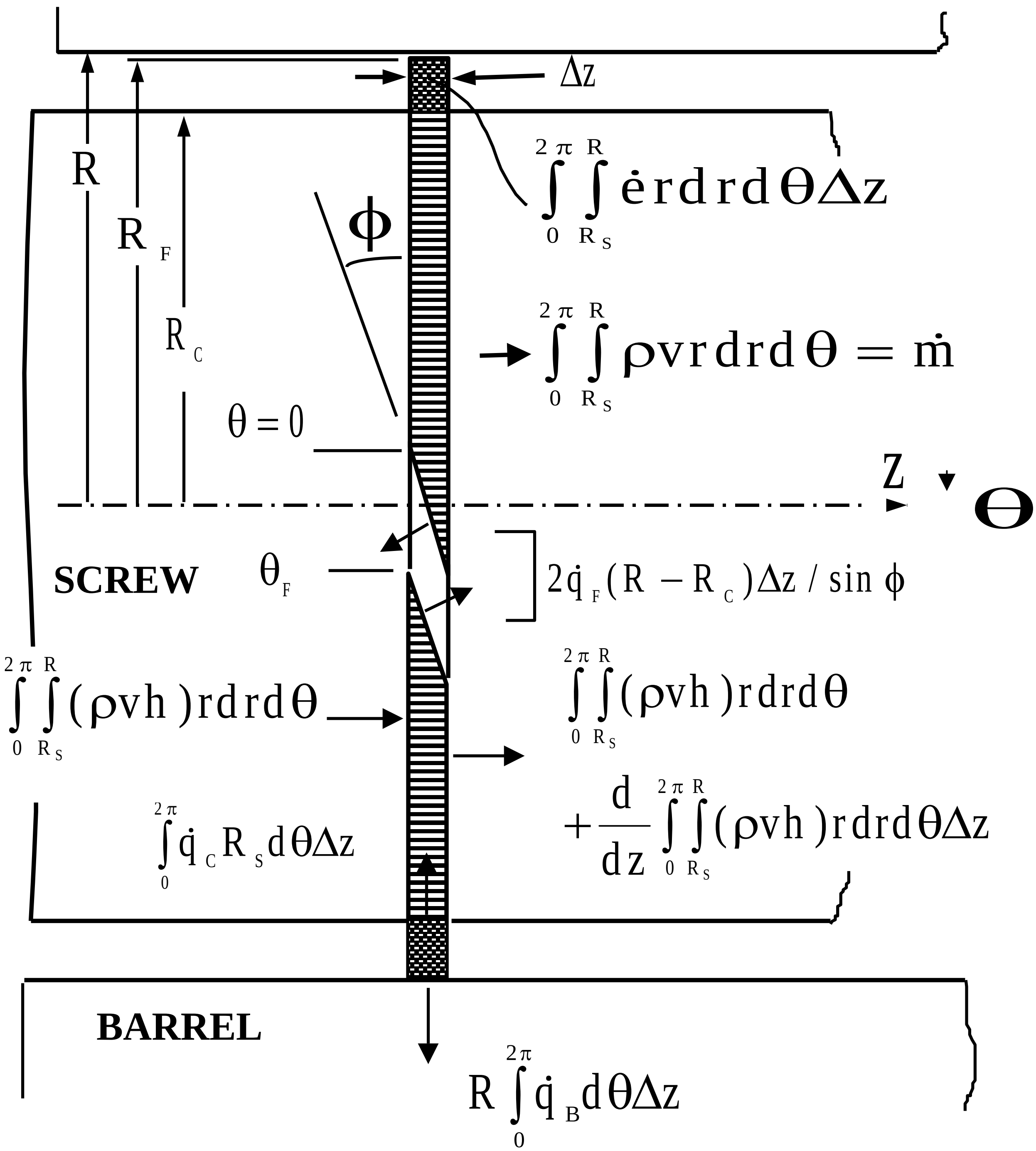

$$R_S = \text{stepwise}$$

$$R_S(z) = R_C(z), 0 \le \theta \prec \theta_F$$

$$R_S(z) = R_F(z), \theta_F \le \theta \le 2\pi$$

Figure 2. Energy Balance for the Annular Channel Segment. Flight clearance is included.

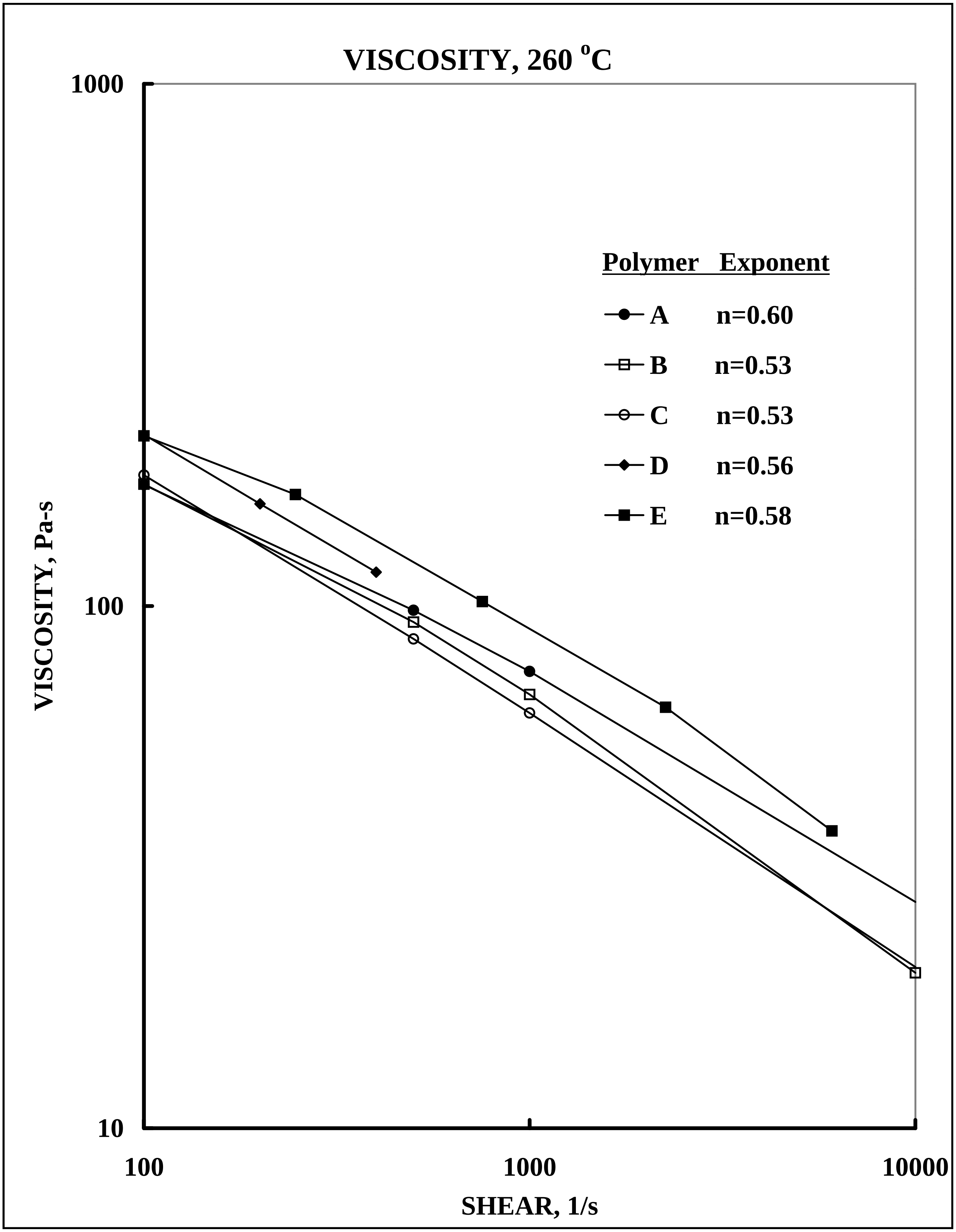

Figure 3. Viscosity of the Polyethylenes. Average exponentials for the power-law given as n.

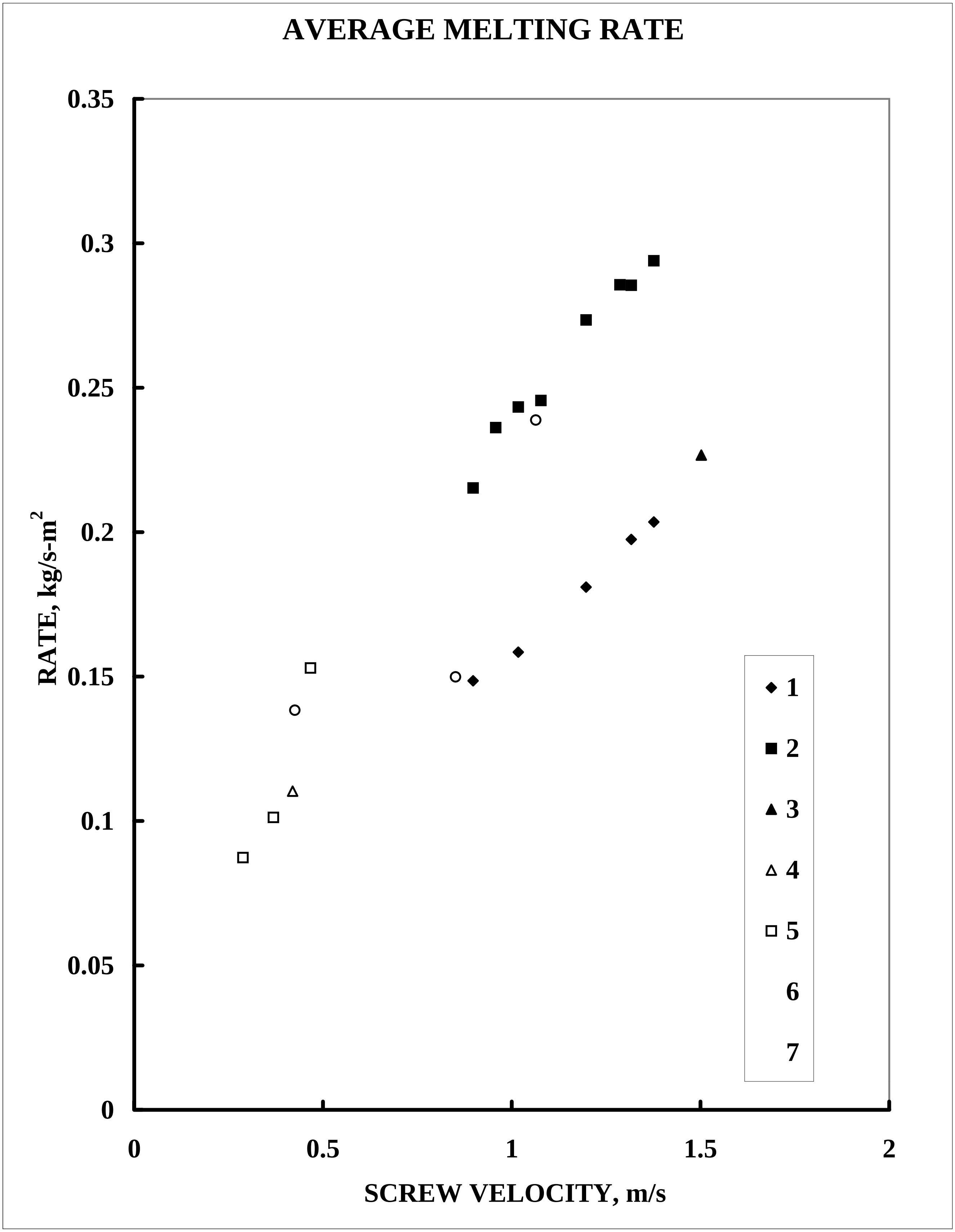

Figure 4. Average Melting Rate for Polyethylene. Each data set is for a different screw and different polyethylene, but all had similar viscosities. Barrel zones were above 220 ^{o}C, except Tadmor [1].

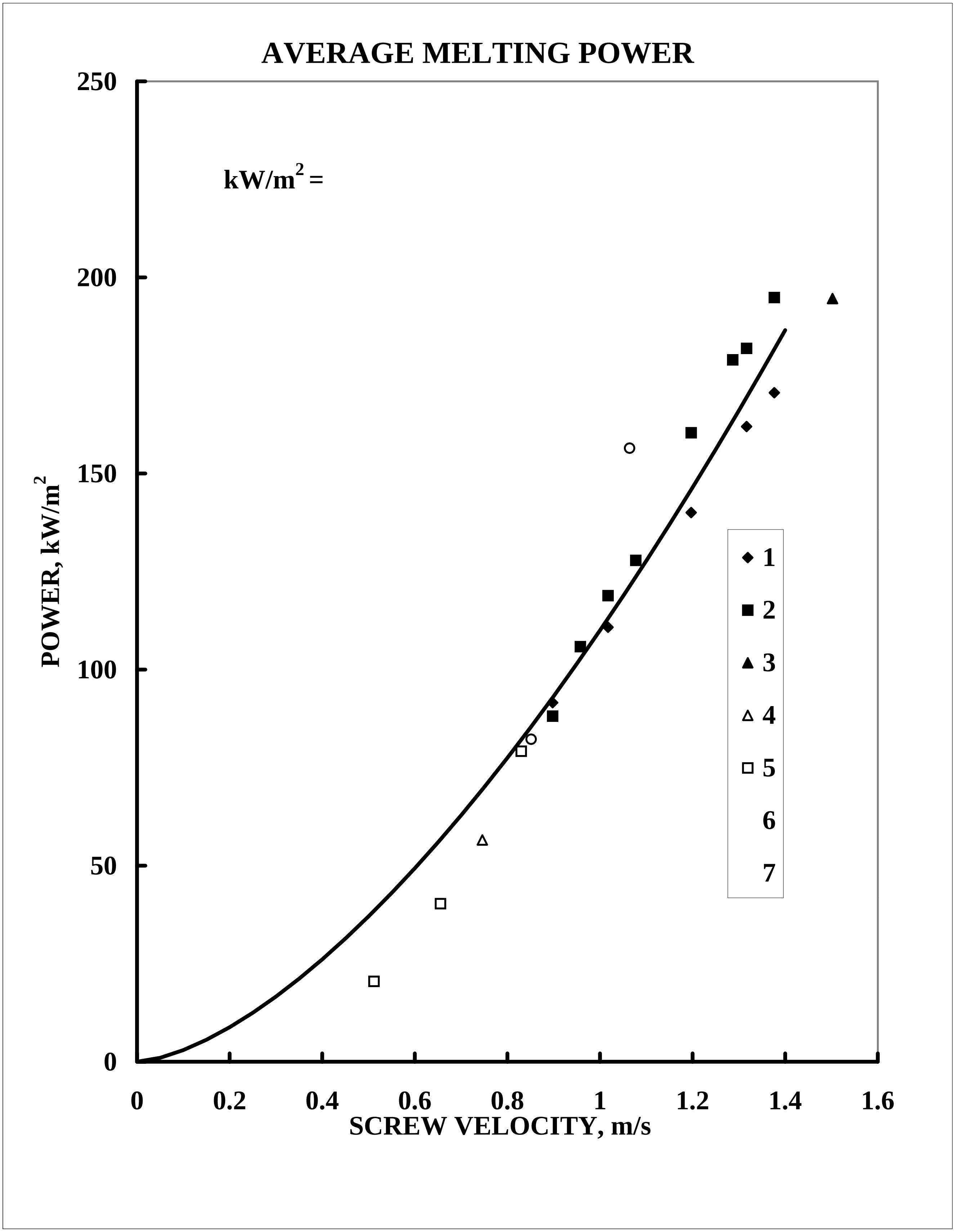

Figure 5. Melting Power for Polyethylene versus Screw Velocity.

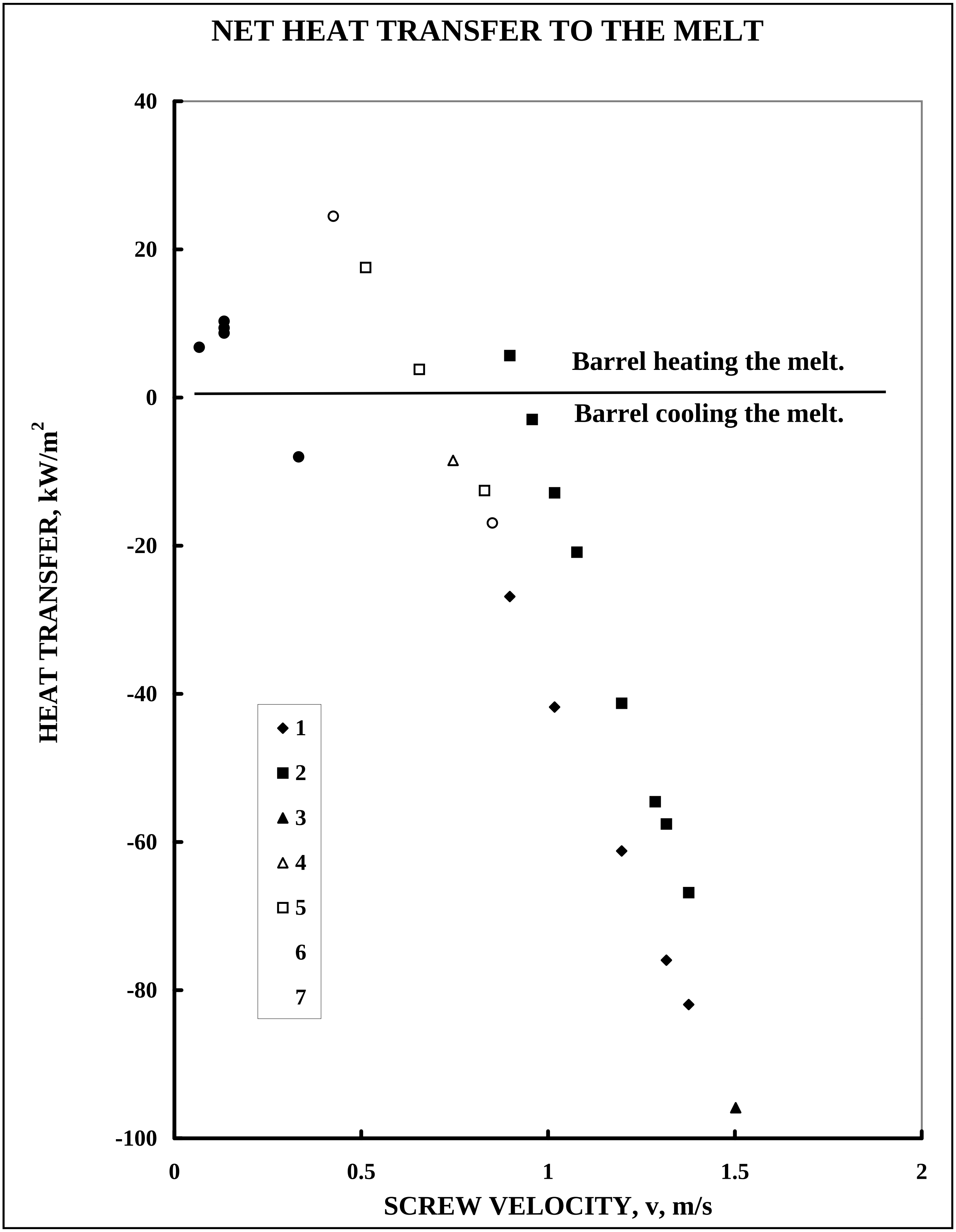

Figure 6. Net Heat Transfer to the Melt. The autogenous velocities, v_0, in the table in the text are interpolations for zero heat transfer.

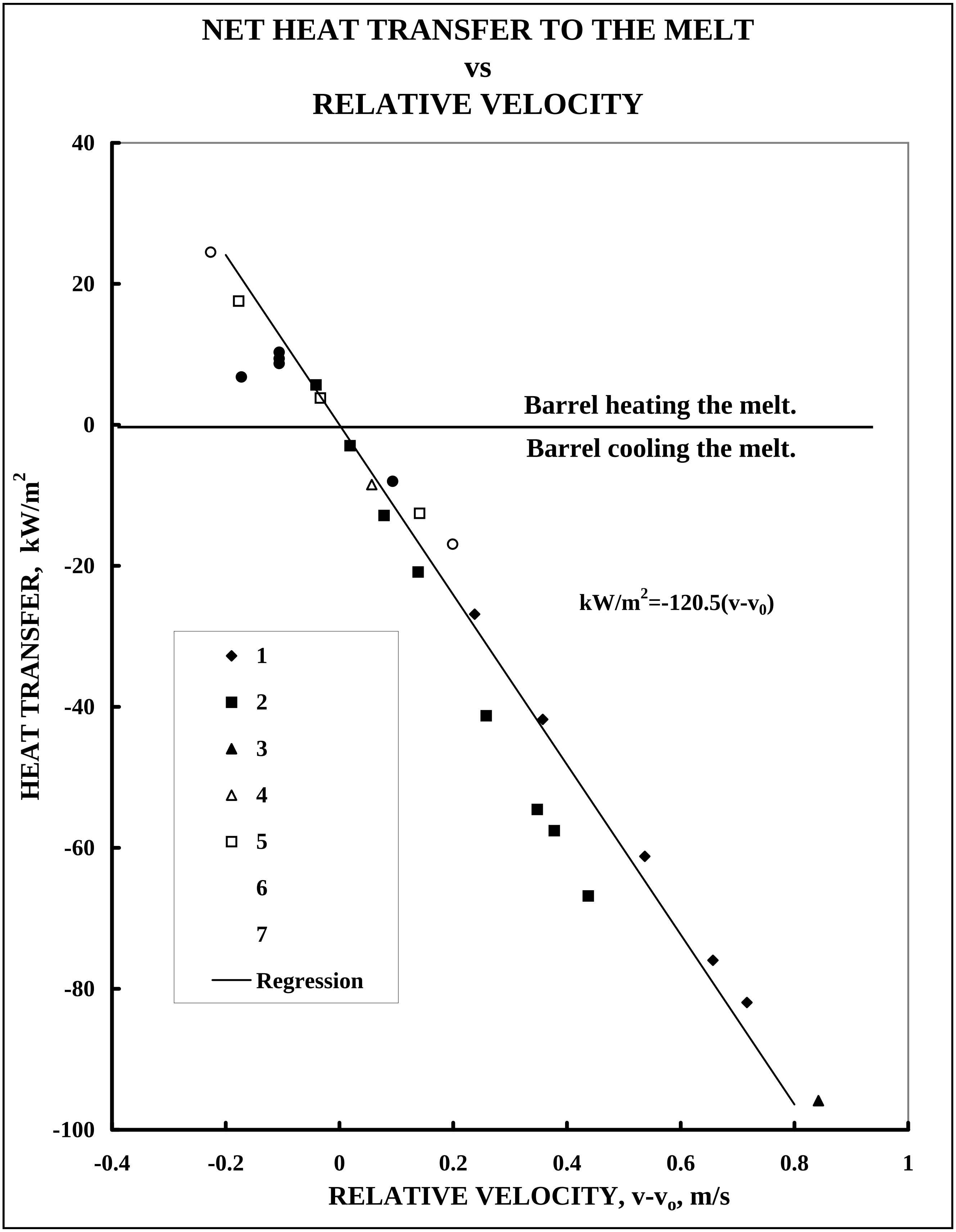

Figure 7. Heat Transfer from the Barrel to the Melt.

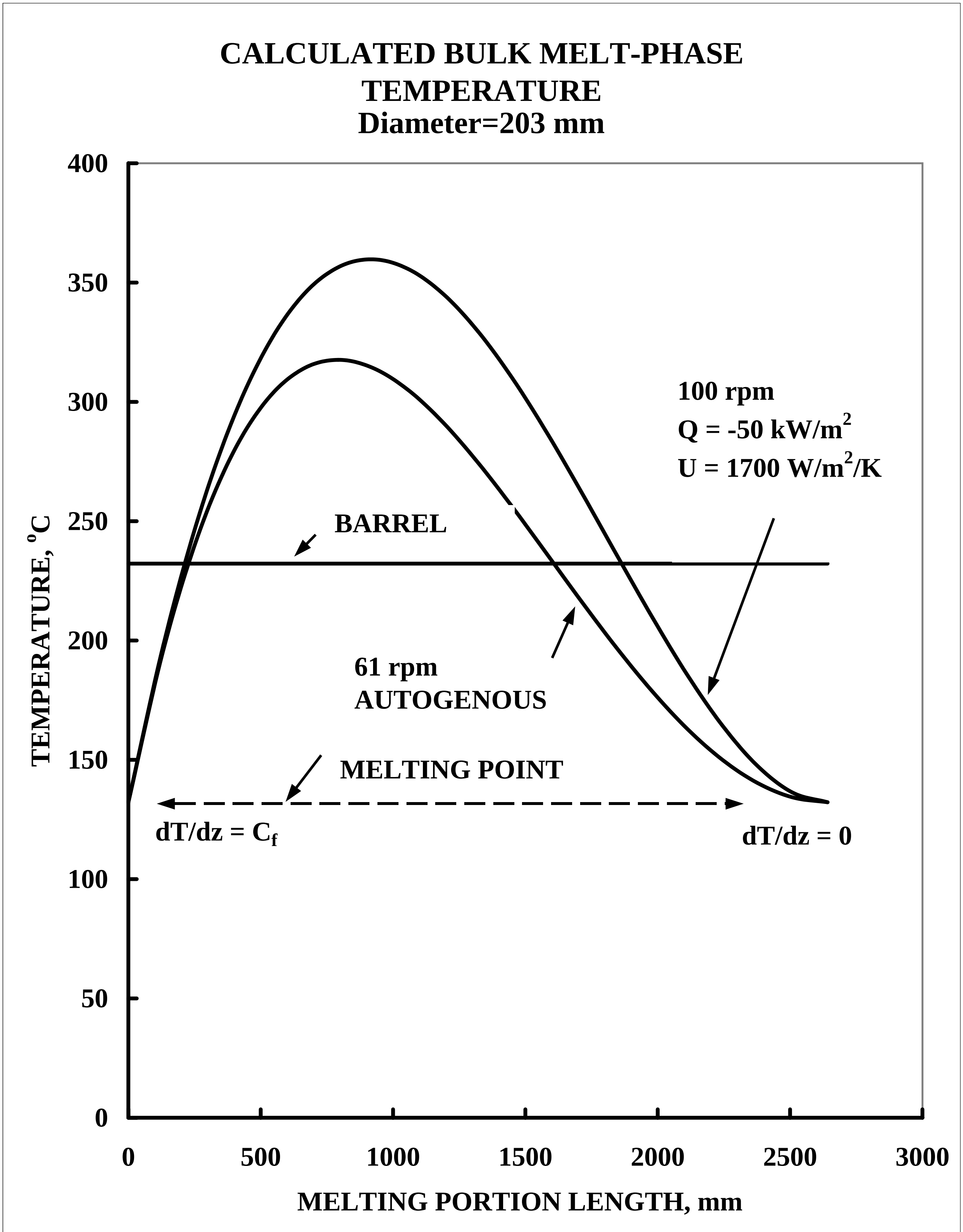

Figure 8. Calculated Bulk Melt-Phase Temperature versus Length. A fourth-order polynomial is assumed and integrated to give the required heat transfer. It is consistent with melt temperature and gradient at each end of the melting portion.